AIAA-2003-6732
MDO of a Blended-Wing-Body Transport Aircraft with Distributed Propulsion

Andy Ko, L.T. Leifsson, J.A. Schetz,
W.H. Mason and B. Grossman
Virginia Polytechnic Institute and State University
Blacksburg, VA

and

R.T. Haftka
University of Florida
Gainesville, FL

AIAA's 3rd Annual Aviation Technology, Integration, and Operations (ATIO) Technical Forum
17-19 November 2003 / Denver, CO

MDO of a Blended-Wing-Body Transport Aircraft with Distributed Propulsion

Andy Ko*, Leifur T. Leifsson†, William H. Mason§, J.A. Schetz‡ and Bernard Grossman¶
Multidisciplinary Analysis and Design Center for Advanced Vehicles
Virginia Polytechnic Institute and State University
Blacksburg, VA 24061-0203

and

Raphael T. Haftka#
Department of Mechanical and Aerospace Engineering,
University of Florida
Gainesville, Florida, 32611-6250

A distributed propulsion concept for aircraft is considered. The concept involves replacing a small number of large engines with a moderate number of small engines and ducting part of the engine exhaust to exit out along the trailing edge of the wing. Models to describe the effects of this distributed propulsion concept were formulated and integrated into an MDO formulation. The most important effect modeled is the impact on the propulsive efficiency when there is blowing out of the trailing edge of a wing. An increase in propulsive efficiency is attainable with this arrangement as the trailing edge jet 'fills in' the wake behind the body, improving the overall aerodynamic/propulsion system, resulting in an increased propulsive efficiency. Other models formulated include the effect of the trailing edge jet on the induced drag, longitudinal control through thrust vectoring of the trailing edge jet, increased weight due to the ducts, and thrust losses within the ducts. When applied to a Blended-Wing-Body (BWB) multidisciplinary design optimization formulation, the distributed propulsion BWB aircraft shows a 5.4% takeoff gross weight advantage over a conventional propulsion BWB aircraft. This savings is mainly due to the effect of the trailing edge jet on the induced drag and the increased propulsive efficiency.

Nomenclature

AR	Aspect ratio
c	Chord length
C_{Di}	Induced drag coefficient
$C_{Di-\text{Dist. Prop.}}$	Distributed propulsion induced drag coefficient
C_J	Jet momentum flux coefficient $= \frac{J}{\frac{1}{2} r U_\infty^2 S_{ref}}$
C_L	Lift coefficient
J	Jet thrust
L/D	Lift to drag ratio
S_{ref}	Wing planform reference area
sfc	Thrust specific fuel consumption
t	Airfoil thickness
T/W	Thrust to weight ratio
$TOGW$	Takeoff gross weight
$U_¥$	Freestream velocity
V_{min}	Minimum velocity at approach
W/S	Wing loading
a	Angle of attack
h_P	Froude propulsive efficiency
h_t	Engine internal thermal efficiency
k_1	*sfc* factor
L	Wing quarter chord sweep angle
t	Jet flap deflection angle
r	Density at altitude

*Member AIAA
† Graduate Student, Student Member AIAA
§ Professor, Associate Fellow AIAA.
‡ Fred D. Durham Endowed Chair, Fellow AIAA.
¶ Professor, currently Vice President, Education, National Institute of Aerospace, 144 Research Drive, Hampton, VA 23666, Fellow AIAA.
# Distinguished Professor, Fellow AIAA

1. Introduction

Multidisciplinary Design Optimization (MDO) has been receiving increased interest in the aerospace industry as a valuable tool in aircraft design [1],[2],[3]. The use of MDO in conceptual and preliminary design of innovative aircraft concepts is but one application where it provides the designer with better insight into the coupled nature of different aerospace disciplines related to aircraft design. In a general MDO aircraft design framework, different analysis modules or their surrogates representing the different disciplines such as structures and aerodynamics, are coupled with an

optimizer to find an optimum design subject to specified design constraints. This provides a means of designing planes requiring tightly coupled technologies.

This paper describes the use of an MDO framework to design a distributed propulsion Blended-Wing-Body (BWB) aircraft [4]. The BWB is a unique tailless aircraft. The high level of integration between the wing, "fuselage", engines, and control surfaces inherent in the BWB design allows it to take advantage of the synergistic nature between the different aircraft design disciplines resulting in an aircraft with better performance than a conventional design. Figure 1 shows a BWB concept with conventional propulsion. With the distributed propulsion concept integrated into the BWB aircraft design, MDO will be used to identify the advantages of this aerodynamics-propulsion integration and highlight its benefits.

Figure 1: The Blended-Wing-Body aircraft with a conventional propulsion arrangement. *NASA Fact Sheet.*

2. The Distributed Propulsion concept

The idea of using distributed-propulsion has been suggested with the objective of reducing noise [5]. Distributing the propulsion system using a number of small engines instead of a few large ones could reduce the total propulsion system noise. There are other potential benefits of distributed-propulsion. One advantage is its improved safety due to engine redundancy. With numerous engines, an engine-out condition is not as critical to the aircraft's performance in terms of loss of available thrust and controllability. The load redistribution provided by the engines has the potential to alleviate gust load/flutter problems, while providing passive load alleviation resulting in a lower wing weight. There is also the possible improvement in affordability due to the use of smaller, easily-interchangeable engines.

One suggested distributed propulsion arrangement is to place an array of small engines distributed along the wings and/or around the fuselage under cowls as depicted schematically in Figure 2. We find this arrangement to be unattractive. The reason is the basic conflict between the axisymmetric geometry of jet or propeller engines and the planar space under the cowl. If the engines are turbojets, little additional air will be entrained to flow under the cowl resulting in poor system propulsive efficiency. If the engines are turbofans, the flow in the irregular spaces under the cowl and surrounding the fans will have high drag and will not contribute to propulsion. Thus, we have rejected further consideration of this arrangement. Rather, we have selected a concept that ducts part of the exhaust from a moderate number of wing mounted engines out of the trailing edge across part or all of the span of the wing. Such a concept could be employed as a seamless high-lift system, dispensing with conventional high-lift systems that are major sources of noise. Figure 3 shows two wing cross sections illustrating this concept. Exhausting out the trailing edge of the wing is similar to jet wing and jet flap concepts.

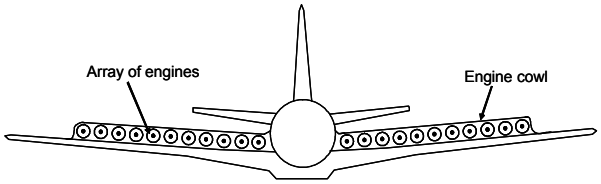

Figure 2: Front view schematic of a distributed-propulsion configuration.

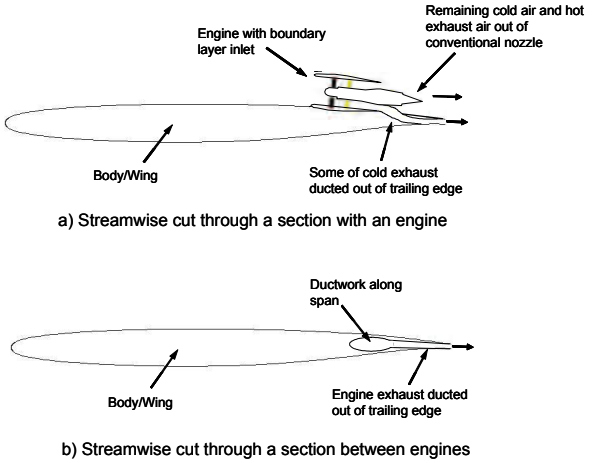

Figure 3: Drawing of wing streamwise cross sections through a location with an engine and a location between engines of the distributed-propulsion concept wing proposed in this paper.

The jet wing concept can be described as an arrangement on a wing where a thin sheet of air from the engine is ejected out of a slot near or at the trailing edge. This utilizes the available power of the engine for thrust and lift augmentation. The jet flap is an arrangement that ejects a thin sheet of high velocity air with a downward inclination out of a slot near or at the trailing edge to obtain high lift. Its application is associated with the generation of powered or high lift capabilities. While both concepts are similar in the sense that air from the engine is ejected out of the trailing edge of the wing. The difference lies in their

application. The jet flap concept involves a large downward deflection of the jet sheet at an angle with respect to the free stream, usually in the context of STOL (Short takeoff and landing) aircraft configurations. The jet wing concept does not usually employ a deflection in the angle of the jet sheet. Two experimental aircraft demonstrated these concepts in flight [6],[7].

The distributed propulsion concept investigated here is a hybrid of the jet wing, jet flap and conventional propulsion concepts. While the jet exhausted out of the trailing edge will not be deflected at high angles during large portions of the aircraft's mission (jet wing concept), it will be deflected at a modest angle to replace conventional flap systems and elevons (jet flap concept). Unlike both the jet wing and jet flap concept, the distributed propulsion concept only ducts part of the engine exhaust out of the trailing edge, with the remaining exhaust using conventional nozzles.

3. Distributed Propulsion Models

3.1. Propulsive efficiency

Kuchemann suggested in 1938 [8][*] that an improvement in propulsive efficiency could be achieved with the jet wing concept. Propulsive efficiency is improved because the jet exiting the trailing edge of the wing 'fills in the wake' behind the wing. This approach is commonly implemented in ships and submarines, having a streamlined axisymmetric body (neglecting the sail and the control surfaces) and a single propeller on the axis. Although the wake is not perfectly filled, this arrangement tends to maximize the propulsive efficiency of the entire system [9]. It is expected that a similar improvement in propulsive efficiency can be achieved with a distributed-propulsion configuration that ducts some of the engine exhaust out of the trailing edge of the aircraft. A mathematical assessment of this hypothesis can be found in reference [10] and [11].

To illustrate our approach to distributed propulsion we consider a two-dimensional, non-lifting, self-propelled vehicle with an engine as shown in Figure 4. The wake of the body is taken as independent of the jet from the engine. For the system to be self-propelled, the drag associated with the velocity deficit due to the wake is balanced by the thrust of the engine. The loss in propulsive efficiency is due to any net kinetic energy left in the wake (characterized by the non-uniformities in the velocity profiles) compared to that of a uniform velocity profile. For this case, a typical Froude Propulsion Efficiency for a high bypass ratio turbofan at Mach 0.85 is 80% [12].

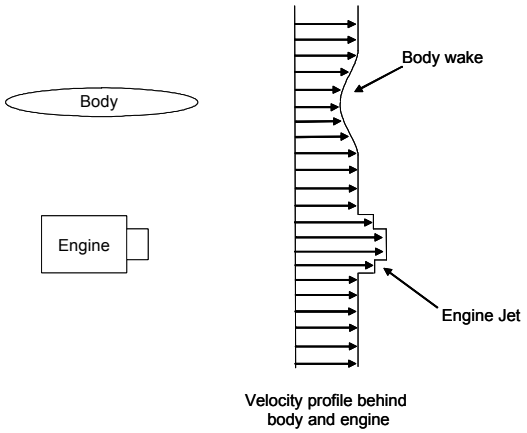

Figure 4: A typical velocity profile behind a body and engine.

Now, consider a distributed-propulsion configuration where the jet and the wake of the body are combined, as shown in Figure 5. In an ideal distributed-propulsion system, the jet will perfectly 'fill in' the wake creating a uniform velocity profile. The kinetic energy added to the flow by the propulsor compared to that of a uniform velocity profile is therefore zero, which results in a Froude Propulsive Efficiency of 100%. In practice, the jet does not exactly 'fill in' the wake but produces smaller non-uniformities in the velocity profile as illustrated in Figure 6. However, this velocity profile will result in a smaller net kinetic energy than that of the case shown in Figure 4, where the body and engine are independent. The efficiency associated with a distributed-propulsion configuration will be bounded by the efficiency of the decoupled body/engine case (nominally at 80%) and the perfect distributed-propulsion configuration of 100%. It should be noted, however, that we have not included the effect the jet has on the pressure distribution of the body. We expect that the jet will entrain the flow over the surface and increase the drag, but this effect is not modeled here.

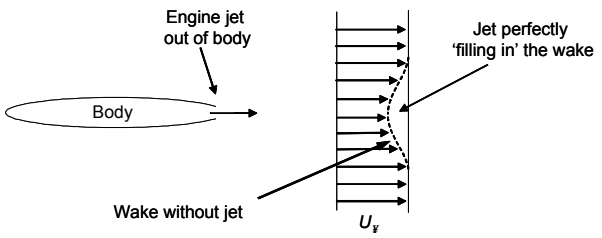

Figure 5: The velocity profile of a perfect distributed-propulsion body/engine system.

[*] The original reference to Kuchemann has been cited to be in: "On the Possiblity of Connecting the Production of Lift with that of Propulsion," *M.A.P. Volkenrode, Reports and Translations* No. 941 – Nov., 1947, APPENDIX I, Kuchemann, D., "The Jet Wing,". However, we were unable to obtain a copy of this reference.

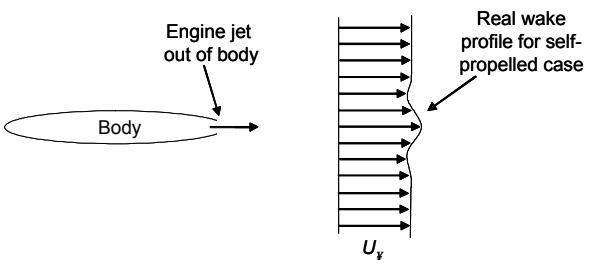

Figure 6: The velocity profile of a realistic distributed-propulsion body/engine system.

Now consider a lifting body with an engine in a distributed-propulsion configuration. In this case, the drag on the system is not only due to the viscous drag but also the drag due to the downwash. This means that the engine jet now 'overfills' the wake. Therefore, even in a perfect system, a 100% Froude Propulsive Efficiency is not attainable. In the perfect system of this configuration, part of the jet would be used to perfectly 'fill in' the wake while the remaining jet would be in the freestream away from the body and used to overcome the induced drag. This arrangement is like that of our distributed propulsion concept illustrated in Figure 3. If the induced drag constitutes about 50% of the total drag (viscous drag + induced drag) as in well designed wings, then the maximum possible increase in Froude Propulsive Efficiency will be half of that in the non-lifting body case, i.e. the Froude Propulsive Efficiency using a nominal high bypass ratio turbofan in a distributed-propulsion setting would be between 80% -90%.

From the above example for a subsonic lifting body, we see that the upper limit of the Froude propulsive efficiency is determined by the ratio of the viscous drag to the total drag. In the same way, for a lifting body in transonic flow, the upper limit of the Froude propulsive efficiency is determined by the ratio of the viscous and wave drag to the total drag. The wave drag is included because the presence of shocks on the body affects the size and shape of the wake behind the wing/body.

In an aircraft design performance assessment, the Froude Propulsive Efficiency can be reflected in the performance in terms of the thrust specific fuel consumption (*sfc*). We should expect that an increase in the Froude Propulsive Efficiency will result in a reduction in *sfc*, improving the aircraft's overall performance.

To relate the Froude Propulsive Efficiency to *sfc*, consider the approximate relation given in Equation (1) by Stinton [13].

$$sfc = \frac{U_\infty}{k_1 h_p h_t} \tag{1}$$

where U_∞ = freestream velocity

k_1 = *sfc* factor. Stinton [13] determined this factor to be 4000 ft-hr/s.

h_p = Froude propulsive efficiency

h_t = the engine internal thermal efficiency

Assuming a constant freestream velocity, *sfc* factor and internal engine thermal efficiency, we can obtain Equation (2).

$$\frac{sfc_1}{sfc_2} = \frac{h_{P2}}{h_{P1}} \tag{2}$$

Hence, given a baseline propulsive efficiency and *sfc*, a new *sfc* can be calculated for an increase in propulsive efficiency.

With the maximum and minimum limits in attainable propulsive efficiency determined, we would expect that only a percentage of this possible increase in propulsive efficiency could be achieved. In implementing this formulation into an MDO framework, we assumed that only 25% of the maximum possible savings in propulsive efficiency could be attained.

3.2. Induced drag

A key theory in describing and analyzing the jet wing is Spence's theory [14],[15],[16]. Spence extended thin airfoil theory to describe airfoil and wing performance with a jet wing in terms of C_J, the jet coefficient. C_J is defined as

$$C_J = \frac{J}{\frac{1}{2} r U_\infty^2 S_{ref}} \tag{3}$$

where J = Jet thrust

r = Density at altitude

S_{ref} = Wing planform reference area

Using Spence's Theory, the induced drag of an aircraft under an elliptical load distribution can be described using Equation (4).

$$C_{Di-\text{Dist. Prop}} = \frac{C_L^2}{pAR + 2C_J} \tag{4}$$

Comparing Equation (4) with the induced drag coefficient equation for a non-jet-winged wing with an elliptical load distribution, we find the addition of the factor $2C_J$ in the denominator that describes the influence of the jet wing on the induced drag of the wing. To implement the effects of the jet on the induced drag of the wing, the induced drag is calculated for the equivalent wing with out the jet, and then corrected with the following ratio.

$$\frac{C_{Di-\text{Dist. Prop.}}}{C_{Di}} = \frac{p\,AR}{p\,AR + 2C_J} \tag{4.5}$$

3.3. Controls/Propulsion Integration

In the distributed propulsion BWB configuration, the elevon controls are replaced with a vectored jet wing control system. This system controls the BWB longitudinally by changing the deflection angle of the jet exiting the trailing edge of the wing.

To estimate the effects of the jet deflection angle on the lift and pitching moment of the aircraft, Spence's theory [14] is used. Spence's two dimensional theory extends the methods of thin-airfoil theory to give a solution for the inviscid incompressible flow past a thin airfoil at a small angle of attack (a), when a thin jet exits the trailing edge at a small deflection angle (t). The method provides an estimate of the lift and pitching moment coefficient of the airfoil in terms of the jet coefficient, C_J. This theory was extended to a three-dimensional wing, corrected to account for wing sweep, to estimate the effects of the jet wing on the lift and pitching moment coefficients. This formulation compared well with a vortex lattice method for various wing planforms at $C_J = 0$. For $C_J > 0$, the formulation produced expected differences with a vortex lattice method (that corresponds to a wing at $C_J = 0$). Details of the formulation and the verification of the results can be found in Reference [10].

3.4. Thrust loss due to Ducting

As a consequence of ducting some of the engine exhaust through the trailing edges of the BWB aircraft, there will be some thrust losses in those ducts. To simulate the duct losses on the portion of the thrust that is exhausted out of the trailing edge, a duct efficiency factor is applied to the that portion of the aircraft thrust. We are currently assuming a 95% duct efficiency.

3.5. Structural/Ducting weight

To simulate the duct weight associated with diverting some of the engine exhaust out of the trailing edges, a duct weight factor is applied to the propulsion system weight. There is a possibility that the duct weight does not scale linearly with the propulsion system weight. It has been suggested that perhaps the duct weight scales more closely with the jet velocity or the mass flow rate of the engine. However, without any compelling information to do otherwise, the distributed propulsion BWB MDO framework scales the duct weight through the use of a factor applied to the propulsion system weight. The nominal factor currently used increases the engine weight by 10%.

4. BWB MDO framework

4.1. BWB Geometric description

The BWB planform is described using a parametric model with a relatively small number of design parameters. Five spanwise stations are used as design variables to define the shape of the planform, see figure 7. The geometric properties at those stations are also design variables. They are chord length (c), airfoil thickness (t) and quarter-chord sweep (L). A straight line wrap method is used to define the properties of the aircraft between the stations.

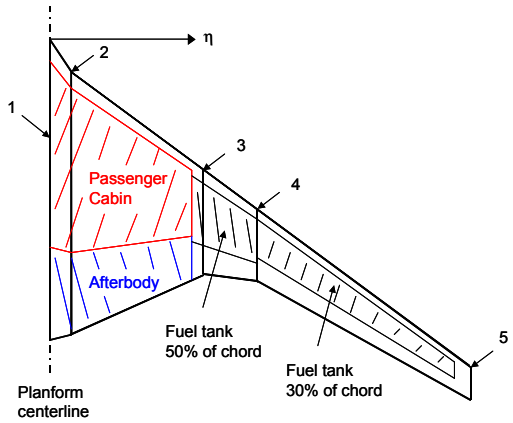

Figure 7: The BWB planform showing the five span stations, location of the passenger cabin, afterbody and fuel tanks.

The passenger cabin is placed at the center inboard section of the BWB. It occupies 60% of the chord behind a 5% leading edge clearance. The remaining rear 35% of the chord in that section defines the afterbody section that houses the aircraft systems, passenger baggage, and emergency exit tunnels. To ensure that there is enough cabin space for the number of passengers carried on the BWB, an average of 10 ft^2 of cabin floor area per passenger is assigned [17]. Currently, a double deck configuration occupies the center section of the passenger cabin, taking up 11% of the cabin span. The remaining cabin area adopts a single deck configuration. Minimum thickness constraints are used to ensure that the passenger cabin is high enough.

The fuel tanks are located in the wing sections outboard of the passenger cabin. They extend to the 95% semi-span location of the wing.

4.2. Aerodynamics

The aerodynamics module models the induced, wave and friction drag of the aircraft. This module evolved from our previous work on truss-braced wing concepts [18].

The induced drag is determined from a Trefftz plane analysis for minimum induced drag [19]. The model also calculates the load distribution on the wing and allows for non-planar surfaces, which provides the capability to model winglets on the BWB.

The wave drag calculation uses the Korn equation [20] to estimate the transonic wave drag of a wing. Simple sweep theory is used to account for sweep. The wing geometry is divided into a number of spanwise strips and the wave drag model estimates the drag as a function of an airfoil technology factor, thickness to chord ratio, section lift coefficient and sweep angle for each individual strip.

The friction drag model is based on applying form factors to an equivalent flat plate skin friction drag analysis. The amount of laminar flow on the BWB is estimated by interpolating results from the Reynolds number vs. sweep data obtained from the F-14 Variable Sweep Transition Flight Experiment [21] and wind tunnel test data from Boltz et al. [22].

4.3. Structures (Wing weight estimation)

The wing weight model used is one that was obtained from NASA Langley's Flight Optimization Software (FLOPS) [23]. This model takes into account the geometry of the individual wing sections, and the number and position of the engines on the wing for load alleviation.

4.4. Weights

The calculation of individual component weights for the BWB is based on the analysis done by Liebeck et al. [17]. With the exception of the wing weight, the equations provided in this NASA contract report were used. Although not used in the results presented in this paper, technology factors can also be applied to the individual weights that are calculated.

4.5. Propulsion

The distributed propulsion arrangement adopted here for the BWB aircraft calls for some of the engine exhaust to be ducted out of the aircraft trailing edge. It also calls for a moderate number of engines (about 8) along the span. This arrangement might place the inlets in the path of the boundary layer developing on the body of the aircraft. Special boundary layer ingestion inlets would be used. However, traditional pylon mounted engines could also be used. For this application, it is assumed that the inlets have the same performance as a regular nacelle inlet on pylons.

The propulsion analysis model calculates the weight, thrust and specific fuel consumption (*sfc*) performance of the engines used on the BWB. The engine weight and thrust models use semi-empirical equations and engine models created by Isikveren [24]. The *sfc* model is based on a GE-90-like engine deck provided by NASA.

4.6. Aircraft performance

The aircraft performance module calculates both aircraft cruise and field performance. For the cruise performance the aircraft range and top of climb rate of climb are calculated. Range is calculated based on the Breguet range equation.

For the field performance, the second segment climb gradient, balanced field length, landing distance, missed approach climb gradient and approach velocity are calculated. The balanced field length calculation is based on an empirical estimation by Torenbeek [25], while the landing distance is determined using methods suggested by Roskam and Lan [26].

4.7. Stability & Control

Only longitudinal control is considered in the MDO formulation. The analysis compares the longitudinal center of gravity (CG) location with the longitudinal control capability of the aircraft through elevons (conventional design) or the thrust vectoring system (distributed propulsion design) based on two assessment criteria. These criteria draw in part on those used by the European MOB project [27]. The two criteria are evaluated at the approach flight phase. Based on a minimum approach velocity of 140 knots, a minimum velocity, V_{min} of 110 knots is used for the longitudinal control evaluation. This is done to provide a 30% safety margin on approach. The two criteria that are used are:

- Maximum elevon deflection boundary at V_{min}
- Maximum angle-of attack boundary at V_{min}

The maximum elevon deflection boundary at V_{min} criteria requires that the CG location of the aircraft should be within limits such that the aircraft elevon trim angles do not exceed the maximum deflection angles of ± 20º. The angle of attack at this condition is that required to provide the required lift during 1*g* flight.

The maximum angle of attack boundary at V_{min} criteria requires that the aircraft CG is at a location such that the angle of attack of the elevon-trimmed aircraft does not exceed the stall angle of attack. Currently, the stall angle of attack is taken to be at 27º.

These two criteria set forward and rear CG limits on the aircraft CG location at four critical weight conditions. Those conditions are at:

- Operational empty weight
- Operational empty weight + Full fuel weight
- Zero fuel weight

- Takeoff gross weight (*TOGW*)

These design conditions are enforced in the MDO framework via the use of optimization inequality constraints.

5. Results

Initially, our BWB model was verified against two published BWB designs. The first was the BWB design by Liebeck et al. [17], published in 1994. The other design, also by Liebeck et al. [28], was published in 1996. The verification was done using the geometry of each of the designs in our BWB MDO code and executing our code in the analysis mode. The results were then compared to those in the publications. The differences for both validation cases were comparable, giving differences in the takeoff gross weight calculations of no more than 8%.

5.1. Mission profile

The mission profile is similar to that used for the BWB design by Liebeck [17], [28]. It uses a 7000 nmi range with a 500 nmi reserve range capability, cruising at a Mach number of 0.85. The passenger capacity of the aircraft is 800 passengers in a three-class configuration. The field performance requires a maximum 11,000 ft takeoff and landing field length. Figure 8 summarizes the design mission profile.

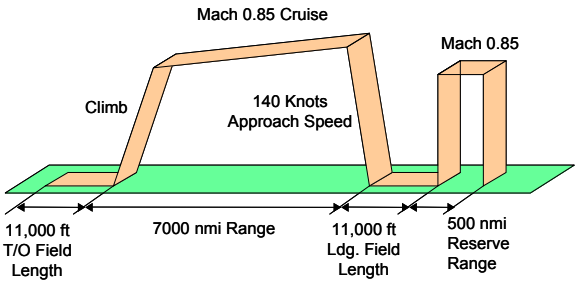

Figure 8: BWB mission profile.

5.2. Optimization results

Two BWB designs were optimized: a distributed propulsion BWB aircraft and a conventional propulsion BWB aircraft used as a comparator.

An eight engine configuration is used for the distributed propulsion BWB aircraft design while the conventional propulsion BWB aircraft has a four engine configuration. For the optimum distributed propulsion BWB design, the engines are evenly spaced inboard of the 70% semi-span location on the wing. Some of the engine exhaust will exit through the trailing edge across the entire span of the aircraft. It is assumed that 25% of the possible savings in propulsive efficiency due to 'filling in the wake' is attainable, and that the ducts used to divert the engine exhaust out the trailing edge have an efficiency of 95%. To account for the weight of the ducts, the weight of the propulsion system is increased by 10%. Although no detailed studies have yet been done to determine a nominal value for these parameters, these values are judged to be realistic.

To examine the individual distributed propulsion effects on the BWB design, four additional optimized BWB designs were made. These designs were created by adding each effect individually to the conventional BWB configuration and obtaining an optimum solution. The five distributed propulsion effects that were examined are:

- Number of engines
- Induced drag effects due to the trailing edge jet
- Savings in propulsive efficiency
- Duct efficiency
- Duct weight factor

Table 1 shows the optimization results for both the conventional BWB configuration and distributed propulsion configuration together with the 'intermediate' distributed propulsion configurations.

5.3. Comparison of final designs

Before examining the results in detail, consider Figure 9, which shows graphically the difference in planform shape between the optimum conventional BWB design and the optimum distributed propulsion BWB design. Both designs share similar planform shapes.

Columns 1 and 6 on Table 1 present the results of the conventional BWB optimum and of the distributed propulsion BWB optimum design, respectively. The optimum distributed propulsion BWB design has a 5.4% lighter *TOGW*, partly due to the 19% lighter wing weight. It uses 7.8% less fuel, and has 3% less thrust. Although the cruise *L/D* and *T/W* ratios are similar for both aircraft, the distributed propulsion BWB aircraft has a higher aspect ratio and a smaller wing loading than the conventional BWB aircraft. This could be partially attributed to the larger wing span of 4% and the smaller reference area of the distributed propulsion BWB aircraft. The distributed propulsion BWB aircraft also has a higher average wing sweep angle than the conventional BWB aircraft.

Table 1: Optimum configuration comparisons between the conventional BWB design and the distributed propulsion BWB design and the distributed propulsion BWB design, together with 'intermediate' optimum designs to show the individual distributed propulsion effects. The conventional BWB design in Column 1 is used as the reference design for calculating all the percentage comparisons.

Design number		1	2	3	4	5	6
		Conv. BWB design (4 engines)	**Conv. BWB design (8 engines)**	**Dist. Prop. BWB design (induced drag effects only)**	**Dist. Prop. BWB design (perfect duct eff. & no duct weights)**	**Dist. Prop. BWB design (no duct weights)**	**Distributed Propulsion BWB design**
Parameters							
Number of engines		**4**	8	8	8	8	**8**
Distributed propulsion factor		**NA**	NA	0.00	0.25	0.25	**0.25**
Duct efficiency		**NA**	NA	1.00	1.00	0.95	**0.95**
Duct weight factor		**NA**	NA	1.0	1.0	1.0	**1.1**
Optimized Design Variable Values							
h	**Root**	**0.000**	0.000	0.000	0.000	0.000	**0.000**
	Section 2	**0.037**	0.039	0.036	0.037	0.037	**0.031**
	Section 3	**0.424**	0.411	0.363	0.380	0.380	**0.377**
	Section 4	**0.548**	0.575	0.495	0.499	0.517	**0.498**
	Tip	**1.000**	1.000	1.000	1.000	1.000	**1.000**
Chord (ft)	**Root**	**143.6**	142.7	144.7	145.9	145.8	**146.2**
	Section 2	**137.8**	136.8	138.6	140.1	139.8	**141.3**
	Section 3	**37.4**	45.6	46.8	40.3	43.0	**41.7**
	Section 4	**21.6**	21.6	22.5	22.0	21.6	**22.2**
	Tip	**7.6**	7.5	7.2	7.1	7.2	**7.1**
t/c	**Root**	**0.18**	0.18	0.18	0.17	0.18	**0.18**
	Section 2	**0.16**	0.16	0.16	0.16	0.16	**0.16**
	Section 3	**0.14**	0.14	0.15	0.16	0.16	**0.16**
	Section 4	**0.14**	0.14	0.13	0.14	0.14	**0.13**
	Tip	**0.13**	0.13	0.14	0.14	0.14	**0.14**
Sweep (deg)	**Section 1-2**	**32.55**	33.04	33.43	32.06	33.23	**32.50**
	Section 2-3	**29.57**	30.21	31.73	31.84	32.24	**31.78**
	Section 3-4	**29.66**	29.78	30.79	32.26	32.12	**31.30**
	Section 4-5	**33.99**	34.51	33.67	34.24	35.07	**34.15**
Wing Span (ft)		**329.13**	319.75	345.16	341.63	335.05	**342.24**
Average Cruise Altitude (ft)		**42345**	41136	42570	42049	41929	**42089**
Total Thrust (lbs)		**157782**	153725	151493	146859	152490	**152979**
Fuel Weight (lbs)		**253938**	263278 (3.68%)	240440 (-5.32%)	232611 (-8.40%)	235861 (-7.12%)	**234191 (-7.78%)**
Optimum Results							
TOGW (lbs)		**902942**	**905509 (0.28%)**	**860509 (-4.70%)**	**847252 (-6.17%)**	**850276 (-5.83%)**	**854461 (-5.37%)**
Wing Weight (lbs)		**129702**	124732 (-3.83%)	108137 (-16.63%)	104713 (-19.27%)	103035 (-20.56%)	**105132 (-18.94%)**
Reference Area (ft^2)		**16254**	16320	16397	16125	16093	**16198**
Aspect Ratio		**6.66**	6.26	7.27	7.24	6.98	**7.23**
***W/S* (lbs/ft^2)**		**55.55**	55.48	52.48	52.54	52.83	**52.75**
T/W		**0.175**	0.170	0.176	0.173	0.179	**0.179**
***L/D* @ Cruise**		**31.00**	29.62	31.28	30.85	30.43	**30.93**
Cruise *CL*		**0.27**	0.25	0.26	0.25	0.25	**0.25**

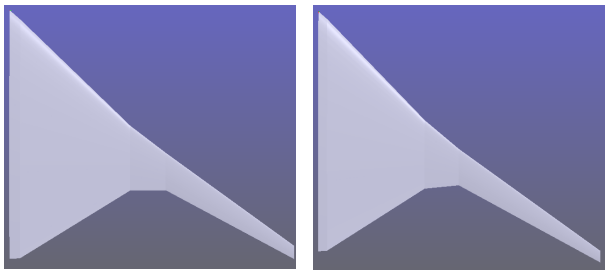

Optimum conventional BWB design

Optimum distributed propulsion BWB design

Figure 9: Comparison of the optimum configuration design of the conventional and distributed propulsion BWB aircraft. Both design figures are not on the same scale.

5.4. Effects of the distributed propulsion parameters

Now consider columns 2 to 5 in Table 1. They show the results of individually adding the distributed propulsion effects to the conventional propulsion BWB design (optimizing for each case) to produce the final distributed propulsion design.

The design in Column 2 increases the number of engines on the conventional propulsion BWB configuration from 4 to 8. This produces an increase in *TOGW* by 0.3%. This is primarily due to an increase in fuel weight of 3.7%. However, there is a decrease in wing weight by 3.8%, mainly due to a 10 ft shorter wing span, which also is responsible for a reduction in aspect ratio. There is also a reduction in the *L/D* ratio bringing it from 31.0 to 29.6.

The design in Column 3 adds the distributed propulsion induced drag effect to the configuration in Column 2. Comparing the results, the induced drag effect is responsible for an almost 5% reduction in *TOGW*. This effect seems to account for the greatest savings in *TOGW* among the distributed propulsion effects. This major reduction in *TOGW* results in a decrease in wing loading (*W/S*) by approximately 3 lbs/ft^2. Part of the reduction in *TOGW* can be accounted for in the reduction of fuel weight by 9% and a decrease in wing weight by 12.8%. The underlying reason for the decrease in weight is in the increase in *L/D* ratio from 29.6 to 31.3. This increase in *L/D* is in part a result of a reduction in induced drag, caused by an increase in wing span and the effect of the trailing edge jet. The increase in wing span (and subsequently the aspect ratio) indicates that the optimizer is capitalizing on the decrease in induced drag gained by the trailing edge jet. In a sense, the effect of the trailing edge jet on the induced drag allowed the optimizer to focus on the aerodynamics of the aircraft as it allowed a greater reduction in *TOGW*.

The design in Column 4 adds the effect of the savings in propulsive efficiency to the design in Column 3. In this configuration, we assumed that 25% of the possible savings in propulsive efficiency can be attained by 'filling in the wake' of the aircraft. This effect further reduced the *TOGW* of the aircraft by 1.5% from the design in Column 3. This is primarily due to a reduction in fuel weight of 3.1% which is a consequence of the improvement in engine efficiency. This is also due to a reduction in wing weight of 2.6% as a result of a 1.7% smaller wing planform area.

The design in Column 5 adds the effect of the duct efficiency to the configuration in Column 4. As expected, when the duct efficiency was reduced from 100% (condition for the design in Column 4) to 95%, the total required thrust increased by 3.6%. This resulted in a *TOGW* increase of 0.34% from the design in Column 4. As a result of the increased required thrust, and therefore the increased weight of the propulsion system, the wing weight increased by 1.3% and the required fuel weight also increased by 1.3% from the design in Column 4. The general aircraft planform and geometric design remained relatively similar.

By comparing the final distributed propulsion BWB design with that on Column 5, we can quantify the effects of the duct weight factor on the distributed propulsion BWB design. Due to the addition of the duct weights, the *TOGW* of the aircraft increased by 0.5%. This is because of an increase in wing weight of 2%. One would expect a greater increase in *TOGW* due to this increase of wing weight. Due to a 2.1% increase in wing span and a 3% drop in *t/c* at the inner wing (section 3) the *L/D* ratio increased by 1.6%. This results in a decrease of 0.7% in required fuel weight and thereby balances the added weight due to the ducts. Except for a small increase in wing span, aspect ratio and average wing sweep, the aircraft remained relatively unchanged geometrically.

6. Conclusions

A model for distributed propulsion has been developed and incorporated into an MDO design formulation. The distributed propulsion concept considered here calls for a moderate number of engines distributed along the span of the wing of the aircraft. Part of the exhaust is ducted through the trailing edge of the wing, while the rest is exhausted through a conventional nozzle. A vectored thrust system applied to the trailing edge jet replaces elevons for longitudinal control and flaps.

The models developed include aerodynamics and propulsion interactions and the longitudinal vectored thrust control system. One of the important models developed is the effect of the trailing edge jet on the propulsive efficiency. An increase in propulsive efficiency can be attained when the engine jet is

exhausted out of the trailing edge of the wing, 'filling in' the wake that is created, and allowing for a better overall aerodynamic/propulsion system. The model considers the maximum and minimum attainable increase in propulsive efficiency for this system, and applies a percentage of that limit to the MDO formulation.

In addition to its effect on propulsive efficiency, the effect of the trailing edge jet on the induced drag is modeled. This model adopts the formulation suggested by Spence [14],[15],[16] where the induced drag is reduced through the jet coefficient, C_J.

Other models include the controls/propulsion integration, thrust losses due to the ducting and the increase in propulsion weight due to the weight of the duct.

The Blended Wing Body (BWB) aircraft was used as a platform to study the distributed propulsion concept. The distributed propulsion models were integrated into a BWB MDO formulation. Our MDO formulation was verified by analyzing previous BWB designs by Boeing.

Two different BWB designs were optimized: a conventional propulsion BWB aircraft and a distributed propulsion BWB aircraft. The results show that the distributed propulsion BWB aircraft has a 5.4% lighter *TOGW* and uses 7.8% less fuel. The distributed propulsion BWB aircraft has a higher aspect ratio design than the conventional BWB design, mostly due to the increased wing span. 'Intermediate' optimum designs reveal that most of the savings in *TOGW* is due to the effect of the trailing edge jet on the induced drag and the increase in propulsive efficiency.

This research shows that the distributed propulsion concept is one that has the potential to provide a savings in *TOGW* and fuel burn.

7. Acknowledgements

The Systems Analysis Branch at NASA Langley supported our work. We would like to acknowledge their help with information, insight and material. We would like to specifically acknowledge William M. Kimmel and Mark Guynn at NASA Langley for their support and help in this work.

8. References

[1] Ashley, H., "On Making Things the Best-Aeronautical Uses of Optimization," *Journal of Aircraft*, Vol.19, No.1, Jan 1982, pp. 5-28.

[2] Sobieszczanski-Sobieski, J., Haftka, R.T., "Multidisciplinary Aerospace Design Optimization: Survey of Recent Developments," *Structural Optimization*, Vol. 14, No. 1, 1997, pp. 1-23

[3] Kroo, I., "MDO Applications in Preliminary Design: Status and Directions," AIAA 97-1408, 1997.

[4] Liebeck, R., "Design of the Blended-Wing-Body Subsonic Transport," 40th AIAA Aerospace Sciences Meeting & Exhibit, AIAA-2002-0002, Reno, NV, Jan 14-17, 2002.

[5] *NASA Aeronautics Blueprint: Toward a Bold New Era in Aviation*, NASA, http://www.aerospace.nasa.gov/aero_blueprint/cover.html.

[6] Solies, U.P., "Flight Measurements of Downwash on the Ball-Bartoe Jetwing Powered Lift Aircraft," *Journal of Aircraft*, Vol. 29, No. 5, Sept-Oct. 1992, pp. 927-931.

[7] Harris, K.D., "The Hunting H.126 Jet Flap Aircraft," AGARD Assessment of Lift Augmentation Devices, Lecture Series 43, Feb., 1971.

[8] Attinello, J. S., "The Jet Wing," IAS Preprint No. 703, IAS 25th Annual meeting, Jan. 28-31, 1957.

[9] *Marine Engineering*, Vol. 1, Society of Naval Architect & Marine Engineers, Ed. Herbert Lee Seward, pp. 10-11.

[10] Ko, Y.-Y. A, "The Multidisciplinary Design Optimization of a Distributed Propulsion Blended-Wing-Body Aircraft," Ph.D. Dissertation, Virginia Polytechnic Institute & State University, April, 2003.

[11] Ko, A., Schetz, J. A., and Mason, W. H., "Assessment of the Potential Advantages of Distributed Propulsion for Aircraft," 16th International Symposium on Air Breathing Engines (ISABE), ISABE-2003-1094, Cleveland, OH, Aug 31- Sept. 5, 2003.

[12] Hill, P. and Peterson, C., *Mechanics and Thermodynamics of Propulsion*, 2nd Ed., Addison-Wesley, New York, 1992.

[13] Stinton, D., *The Anatomy of the Airplane*, 2nd Ed., American Institute of Aeronautics and Astronautics, Reston, VA., 1998, pp153.

[14] Spence, D. A., "The Lift Coefficient of a Thin, Jet-Flapped Wing," *Proceedings of the Royal Society of London,* Vol. 238, Issue 121, Dec. 1956, pp. 46-68.

[15] Spence, D. A., Maskell, E. C., "A Theory of the Jet Flap in Three Dimensions," *Proceedings of the Royal Society of London,* Vol. 251, Issue 1266, June 1959, pp. 407-425.

[16] Spence, D. A., "The Lift Coefficient of a Thin Jet-Flapped Wing. II. A Solution of the Integro-Differential Equation for the Slope of the Jet,"

Proceedings of the Royal Society of London, Vol. 261, Issue 1304, Apr. 1961, pp. 97-118.

[17] Liebeck, R. H., Page, M. A., Rawdon, B. K., Scott, P. W., and Wright, R. A., "Concepts for Advanced Subsonic Transports" NASA CR 4624, Sept. 1994.

[18] Grasmeyer, J.M., Naghshineh, A., Tetrault, P.-A., Grossman, B., Haftka, R.T., Kapania, R.K., Mason, W.H., Schetz, J.A., "Multidisciplinary Design Optimization of a Strut-Braced Wing Aircraft with Tip-Mounted Engines," MAD Center Report MAD 98-01-01, January 1998.

[19] Grasmeyer, J. M., "A Discrete Vortex Method for Calculating the Minimum Induced Drag and Optimum Load Distribution for Aircraft Configurations with Noncoplanar Surfaces," VPI-AOE-242, AOE Department, VPI & SU, Blacksburg, Virginia 24061, Jaunary, 1998.

[20] Malone, B., and Mason, W. H., "Multidisciplinary Optimization in Aircraft Design Using Analytic Technology Models," *Journal of Aircraft*, Vol. 32, No. 2, March-April, 1995, pp. 431-438.

[21] Braslow, A. L., Maddalon, D. V., Bartlett, D. W., Wagner, R. D., and Collier, F. S., "Applied Aspects of Laminar-Flow Technology," *Viscous Drag Reduction in Boundary Layers*, AIAA, Washington D.C., 1990, pp. 47-78.

[22] Boltz, F. W., Renyon, G. C. and Allen, C. Q., "Effects of Sweep Angle on the Boundary Layer Stability Characteristics of an Untapered Wing at Low Speeds," NASA TN D-338, 1960.

[23] McCullers, L. A., *FLOPS User's Guide*, Release 5.81, NASA Langley Research Center.

[24] Isikveren, A. T., "Quasi-Analytical Modelling and Optimisation Techniques for Transport Aircraft Design," Ph.D. Dissertation, Royal Institute of Technology (KTH), Department of Aeronautics, Stockholm, Sweden, 2002.

[25] Torenbeek, E., *Synthesis of Subsonic Airplane Design*, Delft University Press, The Netherlands, 1982.

[26] Roskam, J., and Lan, C.-T.E., *Airplane Aerodynamics and Performance*, DARCorporation, Lawrence, KS, 1997.

[27] Laban, M., Arendsen, P., Rouwhorst, W., and Vankan, W., "A Computational Design Engine for Multi-Disciplinary Optimisation with Application to a Blended Wing Body Configuration," 9th AIAA/ISSMO Symposium on Multidisciplinary Analysis and Opimizationm, AIAA 2002-5446, Atlanta, GA, Sept. 4-6, 2002.

[28] Liebeck, R. H., Page, M. A., Rawdon, B. K., Girvin, R. R., Scott, P. W., Potsdam, M. A., Bird, R. S., Wakayama, S., Hawley, A. V., Rowland, G. T., "Blended-Wing-Body Configuration Control Document (1-26-96) CCD-2," McDonnell Douglas Aerospace, Long Beach, CA, Jan., 1996.